Analytica Chimica Acta 1120 (2020) 1–10

Contents lists available at ScienceDirect

Analytica Chimica Acta

journal homepage: www.elsevier.com/locate/aca

Electrochemical detection of β-lactoglobulin based on a highly selective DNA aptamer and flower-like Au@$BiVO_4$ microspheres

Shengpan Xu [a, b], Benlin Dai [b], Wei Zhao [b], Ling Jiang [c, *], He Huang [a, **]

[a] College of Biotechnology and Pharmaceutical Engineering, Nanjing Tech University, Nanjing, Jiangsu, 211800, PR China
[b] Jiangsu Key Laboratory for Chemistry of Low-Dimensional Materials, Huaiyin Normal University, Huaian, Jiangsu, 223300, PR China
[c] College of Food Science and Light Industry, Nanjing Tech University, Nanjing, Jiangsu, 211800, PR China

HIGHLIGHTS

- The flower-like $BiVO_4$ with peroxidase-like activity were firstly employed to develop electrochemical biosensor.
- A DNA aptamer was used as the recognition group highly selective for β-lactoglobulin.
- A wide detection range from 0.01 to 1000 ng mL^{-1}, with a limit of detection (LOD) of 0.007 ng mL^{-1}.
- The biosensor exhibited excellent selectivity, stability and reproducibility.

GRAPHICAL ABSTRACT

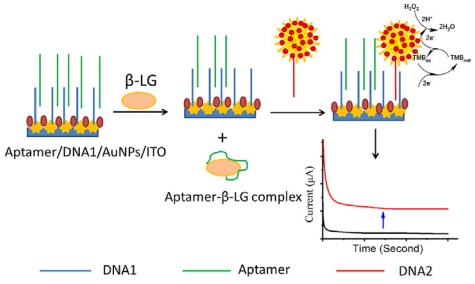

ARTICLE INFO

Article history:
Received 21 February 2020
Received in revised form
23 April 2020
Accepted 26 April 2020
Available online 28 April 2020

Keywords:
β-lactoglobulin
Aptamer
Electrochemical biosensor
$BiVO_4$

ABSTRACT

Beta-lactoglobulin is a natural milk protein and the main cause of infant milk allergy. In this work, a sensitive, selective and inexpensive electrochemical biosensor for the detection of β-lactoglobulin was developed. In this sensor, a DNA aptamer was used instead of an expensive antibody as the recognition group highly selective for β-lactoglobulin. The flower-like $BiVO_4$ microspheres were firstly found to have peroxidase mimic catalytic activity and used to amplify the electrochemical signal. The aptamer can bind β-lactoglobulin and fall off from the working electrode, after which the DNA2/Au/$BiVO_4$ probe can be fixed to the DNA1/AuNPs/ITO working electrode by the hybridization of DNA2 with DNA1. Therefore, a higher concentration of β-lactoglobulin leads to increased fabrication of the DNA2/Au/$BiVO_4$ probe on the surface of the working electrode, and thereby increases the electrochemical signal. This electrochemical biosensor exhibited a wide detection range from 0.01 to 1000 ng mL^{-1}, with a limit of detection (LOD) of 0.007 ng mL^{-1}, which indicates a good potential application in the field of food analysis.

1. Introduction

Cow's milk is one of the most widely consumed foods, and it is not only rich in proteins and calcium, but also rich in lactose, vitamin D, phospholipids, copper, iron and other minerals. Consuming milk and dairy products is beneficial for children's growth and development. However, recent studies have found that proteins in cow's milk can cause serious allergic reactions that

* Corresponding author.
** Corresponding author. College of Biotechnology and Pharmaceutical Engineering, Nanjing Tech University, Nanjing, Jiangsu, 211800, PR China.
E-mail addresses: jiangling@njtech.edu.cn (L. Jiang), biotech@njtech.edu.cn (H. Huang).

https://doi.org/10.1016/j.aca.2020.04.066
0003-2670/

threaten human health, such as adverse reactions in the skin, respiratory tract, gastrointestinal tract, and even the whole body, which has become one of the hot topics in food safety research [1]. For infants and children, β-lactoglobulin in milk is the main allergen. It is abundant, with a concentration of 2–4 g L^{-1} in bovine milk, accounting for approximately 12% of total milk protein and 50% of whey protein [2]. People with allergies must completely avoid food containing allergens. Therefore, it was necessary to develop methods for β-lactoglobulin detection in milk and dairy products to protect public health.

To date, many analytical methods have been developed to detect β-lactoglobulin. Chromatographic methods such as ultra-high-performance liquid chromatography–mass spectrometry [3] and lateral flow immunochromatography [4] were reported. Optical biosensor [5], visualized microarray [6], microcantilever resonator arrays [7] and protein chip method [2] based on immunodetection have been also reported. Commercial enzyme-linked immune sorbent assay (ELISA) kits have been most widely used in reports [8]. In particular, the Chen group published a series of ELISA-based detection methods [9]. These reported methods all have good selectivity. However, chromatography requires expensive equipment and complex sample preparation, while immunoassays usually require expensive antibodies and are time-consuming.

Nucleic acid aptamers have been widely used in biosensors because of their highly selective combination with their target substances [10]. To avoid the use of expensive antibodies, an aptamer targeting β-lactoglobulin was firstly selected in vitro by Zourob et al., and was successfully used for the detection of β-lactoglobulin [11]. Electrochemical methods are also widely used in the detection of various substances [12–14]. The combination of aptamers and electrochemical methods in the construction of biosensors has the advantages of a wide detection range, low limit of detection, good selectivity, portability and low cost [15]. Metal nanomaterials with large specific surface area, excellent electrochemical and catalytic properties have been widely used in the fabrication of electrochemical sensors [16–18]. There are also some studies devoted to the synergy of bimetallic nanomaterials or metal nanomaterials and inorganic two-dimensional nanomaterials to increase electrocatalytic activity [19–21]. One of the nanomaterials with peroxidase-like catalytic activity was often used to amplify the electrochemical signal [22].

In this study, we found firstly that flower-like bismuth vanadate ($BiVO_4$) microspheres have intrinsic peroxidase mimic catalytic activity, which was applied in the construction of an electrochemical biosensor together with a highly selective aptamer to detect β-lactoglobulin (β-LG). In this detection strategy (Scheme 1), the highly selective recognition of β-LG by the DNA aptamer ensures the high selectivity, while the Au nanoparticle-coated indium tin oxide modified conductive glass electrode (AuNPs/ITO) and DNA2/Au@$BiVO_4$ probe with peroxidase-like catalytic activity were combined to amplify the electrochemical signal, which ensures the low limit of detection. This novel electrochemical biosensor is simple and cheap compared to immunoassays, which gives it considerable potential application in real food safety testing.

2. Experimental

2.1. Reagents

Bismuth nitrate pentahydrate ($Bi(NO_3)_3 \cdot 5H_2O$), sodium orthovanadate dodecahydrate ($Na_3VO_4 \cdot 12H_2O$), gold (III) chloride trihydrate ($HAuCl_4 \cdot 3H_2O$), sodium borohydride ($NaBH_4$) and other chemicals used in this work were all of analytical purity and were purchased from Sinopharm Chemical Reagent Co., Ltd. (China). They were used without further purification. All experiments were done using ultrapure water (18 MΩ).

The DNA aptamer and the other two oligonucleotides were synthesized by Sangon Biotech Co., Ltd. (Shanghai, China), with the following sequences:

DNA1: 5′–SH–$(CH_2)_6$-CGTAGGAGCAAGACGCTCACACACGGATGGGCAT-3′
DNA2: 5′–SH–$(CH_2)_6$- ATGCCCATCCGTGTGTGAGCGTCTTGCTCCTACG-3′

Aptamer sequence:

5′-CGACGATCGGACCGCAGTACCCACCCACCAGCCCCAACATCATGCCCATCCGTGTGTG-3′

2.2. Instruments

All the electrochemical measurements were performed on a CHI 660E electrochemical workstation (Shanghai Chenhua Instrument Co. Ltd., China) with a saturated calomel reference electrode and a platinum wire counter electrode. The frequency range of the electrochemical impedance spectra (EIS) was between 0.01 Hz and 100 kHz, with a signal amplitude of 5 mV in the electrolyte containing 5 mM of $Fe(CN)_6^{3-/4-}$ and 0.1 M KCl. The amperometric i-t curve was recorded in 0.1 M sodium-phosphate buffer (pH 6.5) containing 0.5 mM H_2O_2 and 0.5 mM 3,3′,5,5′-tetramethylbenzidine (TMB) with the potential of 0.3 V. The prepared materials were characterized by powder X-ray diffraction (XRD), scanning electron microscopy (SEM) and UV–vis spectroscopy.

2.3. Preparation of aptamer/DNA1/AuNPs/ITO electrode

The preparation of DNA1/AuNPs/ITO was done as described in our previous work [13], with minor modifications as follows. First, the AuNPs were fabricated on the surface of the ITO electrode via potentiostatic electrodeposition in 0.5 mM $HAuCl_4$ solution (get through nitrogen for at least 30 min) under the potential of 0.3 V for 1200 s according to the work of Su et al. [23] with some modification. Then, DNA1 was successfully attached to the AuNPs-modified ITO to form the final DNA1/AuNPs/ITO working electrode. Nonspecific adsorption sites were passivated in 1 mM MCH for 2 h at room temperature. For detailed assembly steps please see the supporting information.

Preparation of the Aptamer/DNA1/AuNPs/ITO was done by adding 10 μL of the aptamer solution (15 μM in 10 mM Tris-HCl, 1 mM EDTA, 50 mM NaCl, pH 7.4) to the surface of the DNA1/AuNPs/ITO electrode and incubating overnight at room temperature. Finally, the prepared Aptamer/DNA1/AuNPs/ITO working electrode was rinsed and stored in tris-acetate buffer (10 mM, pH 8.0) at 4 °C.

2.4. Fabrication of the DNA2/Au@$BiVO_4$ probe

The preparation of flower-like $BiVO_4$ microspheres followed the hydrothermal method of Zhao's group [24]. First, 0.1 mmol $Bi(NO_3)_3 \cdot 5H_2O$ and 0.2 mmol $Na_3VO_4 \cdot 12H_2O$ were dispersed in 40 mL water by ultrasonication, and then sealed in a 80 mL autoclave flask. After 8 h of reaction at 160 °C, the mixture was washed twice with ethanol and water. Finally, the flower-like $BiVO_4$ microspheres were obtained after drying overnight at 60 °C in a vacuum oven.

Preparation of DNA2/Au@$BiVO_4$ was done by adding 5 mL of ice-cold $NaBH_4$ (10 mM) dropwise to 200 mL $BiVO_4$ (0.1 mg mL^{-1}, containing 0.1 mM $HAuCl_4$) under vigorous stirring. After an hour of

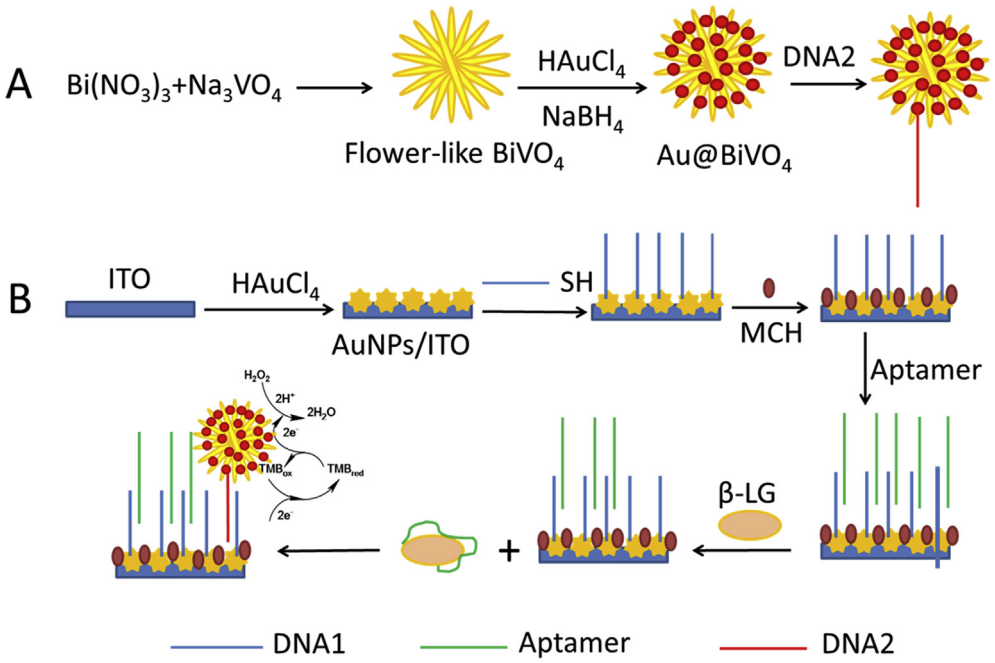

Scheme 1. Schematic of the β-LG detection strategy. (A) Preparation of the DNA2/Au@$BiVO_4$ probe; (B) Fabrication of the biosensor and electrochemical detection of β-LG.

stirring on ice, Au@$BiVO_4$ was collected by centrifugation at 10,000 rpm for 5 min, and then dried for further use. Afterwards, 100 μL mixture (15 μM DNA2, 0.5 mM TCEP) was added to 1 mL Au@$BiVO_4$ (0.1 mg mL^{-1}, 25 mM Tris-acetate buffer pH 8.0), and incubated overnight in the dark at room temperature. The prepared DNA2/Au@$BiVO_4$ probe was washed twice with Tris-acetate buffer (10 mM, pH 8.0), re-dispersed in 1 mL Tris-acetate buffer (10 mM, pH 8.0), and stored at 4 °C until further use.

2.5. Detection of β-LG

For detection, samples comprising 10 μL of different concentrations of β-LG in water were pipetted onto the surface of the Aptamer/DNA1/AuNPs/ITO working electrode. After 80 min of reaction, the working electrode was rinsed with Tris-acetate buffer (10 mM, pH 8.0) to remove the aptamer-β-LG complex. Then, 10 μL of the DNA2/Au @ $BiVO_4$ probe (10 mM Tris-HCl, 1 mM EDTA, 50 mM NaCl, pH 7.4) was added to the electrode surface and incubated for 1.5 h at room temperature, after which it was rinsed and immediately used for electrochemical amperometric i-t curve recording under the potential of 0.3 V (0.5 mM TMB, 0.5 mM H_2O_2, 0.1 M PB, pH 6.5).

3. Results and discussion

3.1. Characterization of the AuNPs/ITO electrode

The bare ITO and AuNPs/ITO electrode were characterized by SEM and EDS analysis. Compare Fig. 1(A) with Fig. 1(B), we found that the surface of the ITO electrode was successfully modified by Au agglomerates with a size of 500 nm assembled by Au nanoparticles via electrodeposition (Fig. 1(C)). It can be seen from Fig. 1(D) that the atomic ratio of In: Sn in the indium tin oxide film on the commercial ITO surface is about 9: 1, while other elements mainly come from glass. The EDS analysis of AuNPs/ITO electrode (Fig. 2) was also proved that the AuNPs/ITO electrode was successfully fabricated with an atomic ratio of Au: In in order of 1: 5.

The rough surface of AuNPs can provide a large specific surface area and abundant active sites for the adsorption of DNA. The effective surface area (A) of the ITO electrode was estimated via CV carried out in the electrolyte containing 5 mM of $Fe(CN)_6^{3-/4-}$ and 0.1 M KCl (Fig. 8(A)) according to the Randled-Sevcik equation [25]:

$$I_p = 2.69 \times 10^5 n^{3/2} A D^{1/2} v^{1/2} C$$

Where, I_p is the current maximum in amps (4.172, 7.373×10^{-4} A for bare and AuNPs modified ITO electrode), n is the number of electrons transferred in the redox event (1), A is the electrode area in cm^2, D is the diffusion coefficient in $cm^2\ s^{-1}$ (6.7×10^{-6}), v = scan rate in V s^{-1} (0.1) and C is the concentration in mol cm^{-3} (5.0×10^{-6}). By calculation, the effective surface area (A) of the AuNPs/ITO electrode was 0.670 cm^2, 1.78-fold that of the bare ITO electrode (0.379 cm^2).

3.2. Characterization of flower-like $BiVO_4$ microsphere and Au@$BiVO_4$

The morphologies of the prepared $BiVO_4$ microspheres were characterized by SEM (Fig. 3(A)). It is clear that the flower-like $BiVO_4$ microspheres with uniform structure were assembled from $BiVO_4$ nanosheets and were basically consistent with the description in the literature [26]. The XRD pattern (Fig. 4) proved that the as-prepared $BiVO_4$ was in the monoclinic phase with a body-centered structure [JCPDS: 14–0688]. There are two strong peaks at 28.3° and 32.4° corresponding to the (121) and (040) crystal planes, respectively, which demonstrated the successful preparation of $BiVO_4$ microspheres.

The gold nanoparticles were fabricated on the surface of $BiVO_4$ microspheres to increase the conductivity and electrocatalytic activity, and also enable them to adsorb DNA2 on the surface through Au–S chemical bonds. It can be seen from Fig. 3(B) that gold nanoparticles were successfully loaded on the surface of $BiVO_4$ microspheres. The diffraction peaks (38.2°, 44.4°, 64.6°) corresponding to the (111), (200) and (040) crystal planes of the AuNPs (Fig. 4) also confirmed the successful preparation of Au@$BiVO_4$ according to the standard diffraction pattern [JCPDS: 04–0784].

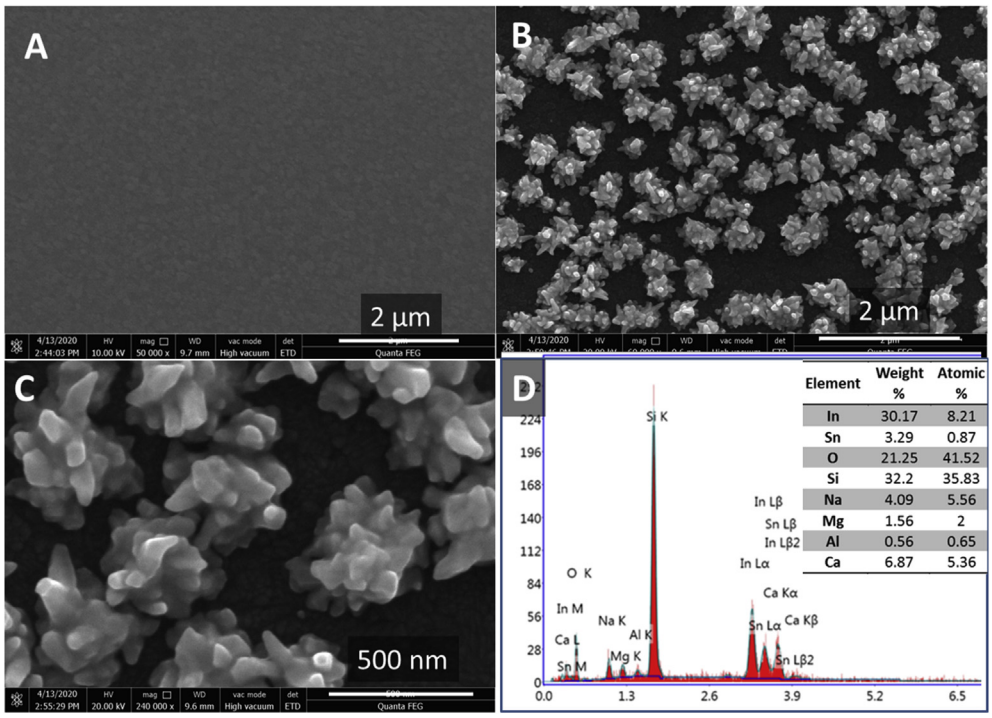

Fig. 1. (A) SEM image of bare ITO; (B) SEM image the AuNPs/ITO electrode (2 μm); (C) SEM image the AuNPs/ITO electrode (500 nm); (D) EDS spectrum of bare ITO.

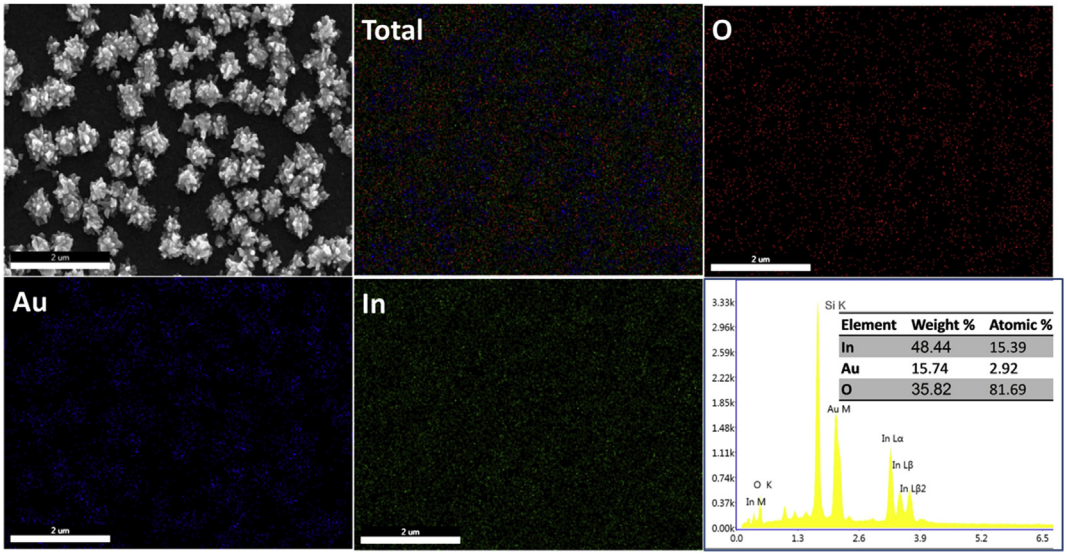

Fig. 2. EDS mapping of the AuNPs/ITO electrode.

Chemical element analysis of the as-prepared material (Fig. 5) was also characterized. The atomic percentage content of Au, Bi, V and O were 4.20%, 16.76%, 16.89% and 62.14% respectively according to the EDS mapping. The atomic ratio of the three atoms (Bi: V: O) was about 1: 1: 4, indicating that the results are credible. This result further confirmed that the AuNPs were well-distributed on the surface of $BiVO_4$.

We made a preliminary investigation of the peroxidase-like catalytic activity of $BiVO_4$ (Fig. 6). In the presence of flower-like $BiVO_4$, the reaction system changed from colorless to blue, meanwhile the characteristic absorption peak of TMBox at 652 nm was also found, which indicated the occurrence of the TMB oxidation reaction. This result proved that $BiVO_4$ indeed has the peroxidase mimic activity and can catalyze the reaction of H_2O_2 with TMB.

3.3. Feasibility of the electrochemical biosensor

The electrochemical CV method was used to detect the electrocatalytic activity of $BiVO_4$. In brief, added 5 μL of a mixed suspension containing 0.5 mg mL^{-1} $BiVO_4$ and 0.05 mg mL^{-1} chitosan dropwise on the surface of the ITO electrode. After drying at room temperature, the $BiVO_4$-modified ITO was performed CV measurement in 0.1 M sodium-phosphate buffer (pH 6.5). As can be seen in Fig. 7, TMB oxidation-reduction peaks were found at

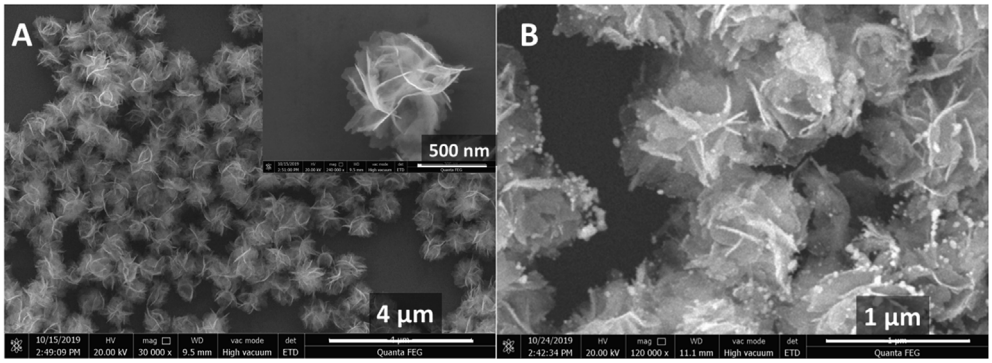

Fig. 3. SEM images of flower-like $BiVO_4$ microspheres (A) and Au@$BiVO_4$ microspheres (B).

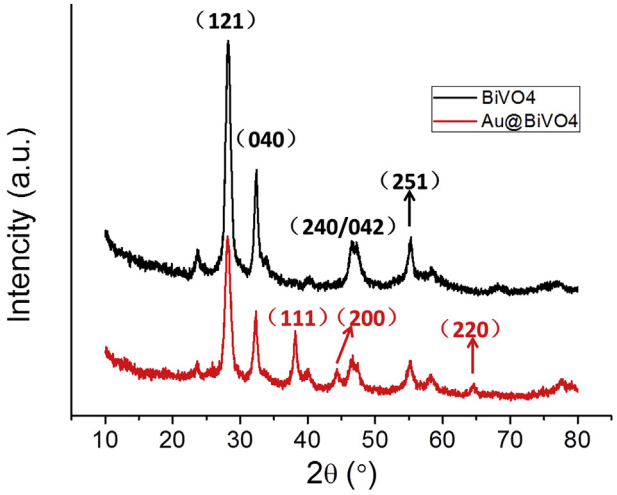

Fig. 4. XRD patterns of the prepared samples.

potential of 0.3 and 0.2 V with $BiVO_4$ attached onto the surface of ITO (Fig. 7d), much larger than the peaks without $BiVO_4$ (Fig. 7c). There were no obvious peaks of the other samples (Fig. 7a and b). This showed that $BiVO_4$ has electrochemical stability and can catalyze the reaction of H_2O_2 with TMB.

The catalytic possible mechanism of $BiVO_4$ was also discussed. According to reference [27], loading gold particles on 2D nanosheets does not affect the peroxidase mimic catalytic activity. Since the prepared $BiVO_4$ is assembled by 2D nanosheets so it will not affect the catalytic activity when loading AuNPs on the surface. $BiVO_4$ is an n-type semiconductor [27]. Under the applied potential, the surface is negative so as to adsorb the positive TMB molecules. Lone pair electrons from the amino group of TMB will transfer to the surface of n-$BiVO_4$ so as to increase electron density and accelerate the electron transfer rate from TMB to H_2O_2, which in turn increases the reaction rate. After H_2O_2 obtains electrons, it generates •OH under weakly acidic conditions (pH 6.5), and further oxidizes TMB to obtain the blue product TMBox. The possible mechanism of catalytic reaction might be depicted as follows [28,29].

$$[BiVO_4]^- + TMB \rightarrow [BiVO_4{*}TMB] + e^-$$

$$H_2O_2 + H^+ + e^- \rightarrow \bullet OH + H_2O$$

$$[BiVO_4{*}TMB] + \bullet OH \rightarrow [BiVO_4]^- + TMBox$$

We also conducted CV and EIS experiments to inspect the assembly process of the working electrode (Fig. 8). It was noting that the peak current of the CV curves was large to the order of 10^{-4} A, and the corresponding resistance was very small, less than 100 Ω. This may due to the low-resistance ITO electrode (6–8 Ω) and large working area of ITO (5 × 3 mm) controlled by platinum electrode holder. The current of the bare ITO electrode was 4.773×10^{-4} A with the corresponding charge-transfer resistance (Rct, 56 Ω). When AuNPs were fabricated on the surface of ITO, the electronic transfer capability was increased, so that the CV signal became larger (7.375×10^{-4} A) and Rct became smaller (23 Ω). However, when DNA1 and the aptamer were sequentially assembled on the surface of Au/ITO, the electronic transfer capability successively declined, with the gradual decrease of CV signal (6.561×10^{-4} A and 4.172×10^{-4} A, respectively) and increase of Rct (40 Ω and 70 Ω, respectively). These results showed that the electrode assembly steps were feasible and successful.

3.4. Optimization of the biosensor

We optimized several conditions during the sensor assembly and detection process. The reaction time with different concentrations of β-LG and aptamer was firstly investigated. As can be seen in Fig. 9(A), the reaction time was somewhat longer with lower concentrations of β-LG. At a low concentration of 0.01 ng mL^{-1}, 80 min was needed to reach the equilibrium. We therefore chose 80 min as the optimal reaction time.

The concentration of DNA1 also investigated (Fig. 9(B)). As the concentration increased, the electrochemical signal increased first and then decreased slightly. It is possible that a too high density of DNA1 attached to the electrode surface hindered the subsequent assembly of the aptamer and the DNA2/Au@$BiVO_4$ probe, so we chose 10 μM as the optimal DNA1 concentration.

Additionally, we inspected the incubation time of the DNA2/Au@$BiVO_4$ probe with the DNA1/Au/ITO working electrode at different concentration of DNA2 (Fig. 9(C)). When the concentration of Au@$BiVO_4$ was 0.1 mg mL^{-1}, the higher the concentration of DNA2 was, the more DNA2 was connected to the surface of Au@$BiVO_4$, and the shorter the incubation time was needed. Considering the economic factors, we chose 15 μM as the optimal concentration of DNA2 since there was not much difference at the concentrations of 15 μM and 20 μM. As can be seen in Fig. 9(C), in the optimal concentration of DNA2, 1.5 h was enough for the hybridization of DNA1 and DNA2.

Finally, the pH value of the detection system was optimized (Fig. 9(D)). As expected, the electrochemical signal was strongest in a weakly acidic buffer, because acidic conditions are conducive to the redox reaction of TMB, while weak acidity and weak basicity are conducive to the stability of DNA. Therefore, pH 6.5 was chosen as the optimal pH value.

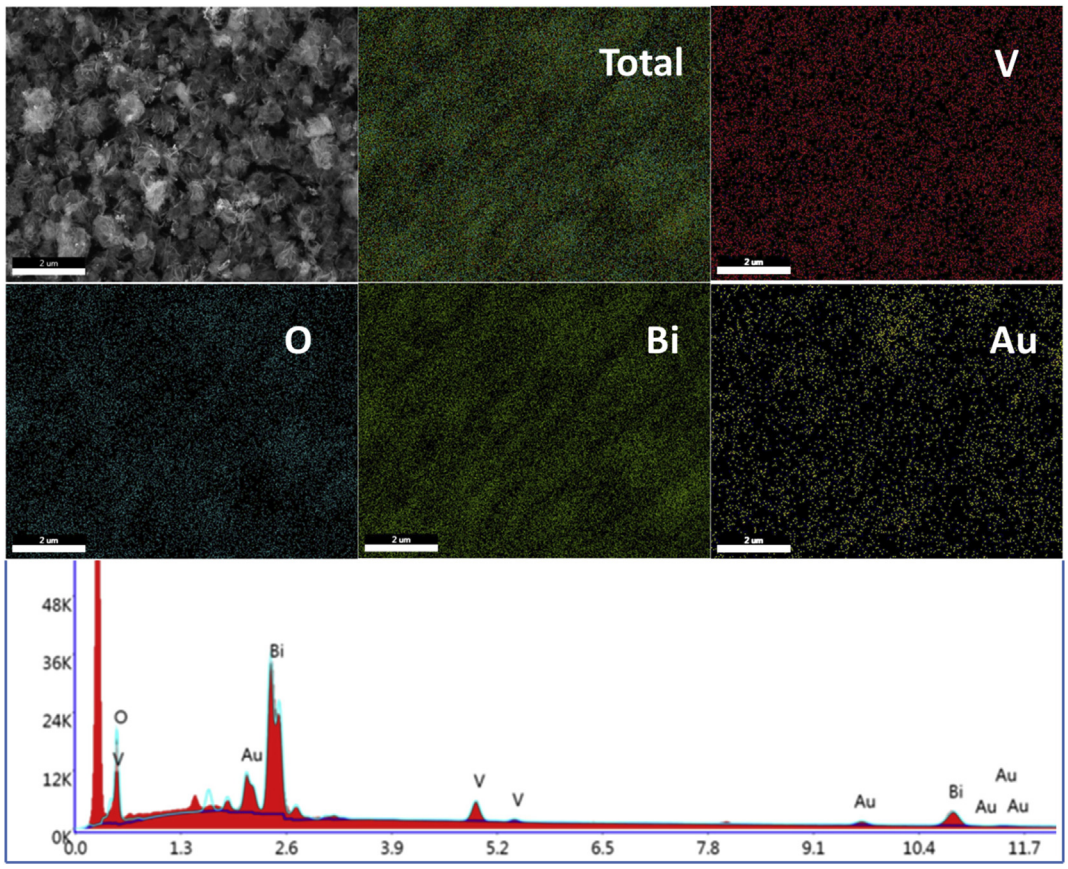

Fig. 5. EDS mapping of Au@$BiVO_4$

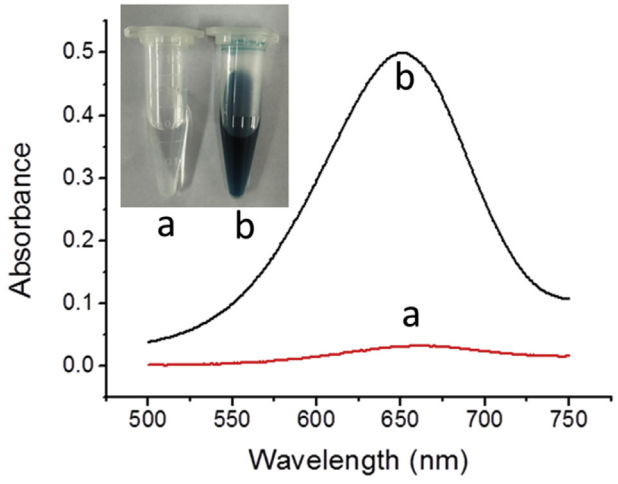

Fig. 6. UV–vis absorbance spectra of (a) 0.5 mM H_2O_2+0.5 mM TMB, (b) 0.5 mM H_2O_2+0.5 mM TMB+0.02 mg mL^{-1} $BiVO_4$. Both reaction mixtures were incubated at room temperature for 30 min (10 mM NaAc-HAc buffer, pH 4.0).

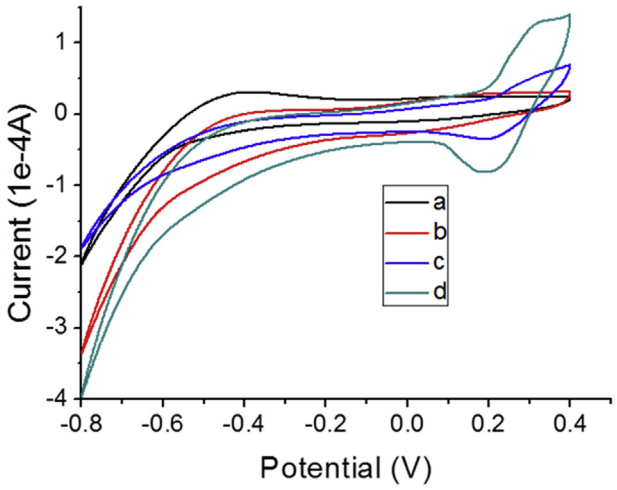

Fig. 7. CVs in 0.1 M sodium-phosphate buffer (pH 6.5) at the scan rate of 100 mv s^{-1}. (a) blank, ITO; (b) 0.5 mM H_2O_2, ITO; (c) 0.5 mM TMB and 0.5 mM H_2O_2, ITO; (d) 0.5 mM TMB and 0.5 mM H_2O_2, $BiVO_4$-modified ITO.

3.5. Detection range and LOD of the biosensor

To test the detection range and LOD of the system, we detected β-LG at different concentrations under the optimal conditions. In brief, after 80 min of reaction between β-LG and the Aptamer/DNA1/AuNPs/ITO working electrode, the aptamer-β-LG complex fell off the electrode so as the DNA2/Au@$BiVO_4$ probe was fabricated on the surface of the electrode through the hybridization of DNA1 and DNA2. At last, electrochemical amperometric i-t curves were recorded under the potential of 0.3 V (0.5 mM TMB, 0.5 mM H_2O_2, 0.1 M PB, pH 6.5). From Fig. 10(A), it is clear that the current signal increased with the concentration of β-LG. This is because β-LG can combine with the aptamer and fall off from the electrode. The higher the concentration of β-LG, the more DNA2/Au@$BiVO_4$ probes will be

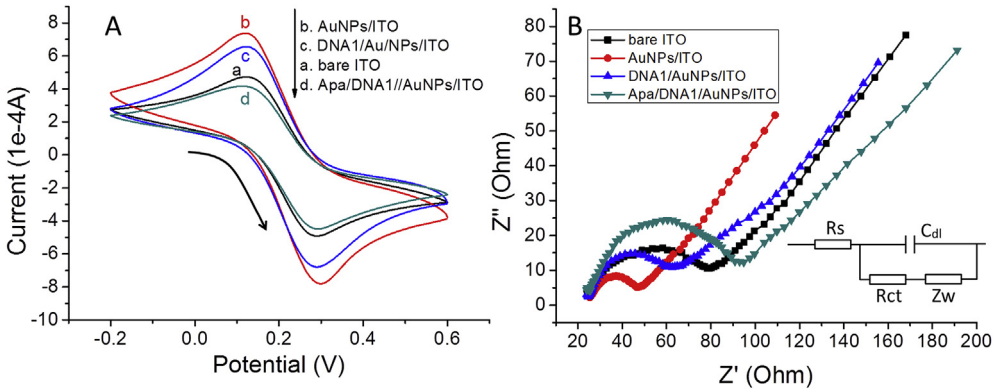

Fig. 8. CV at the scan rate of 100 mv s^{-1} (A) and EIS (B) of the working electrode at different steps during fabrication. Both CV and EIS were carried out in the electrolyte containing 5 mM of $Fe(CN)_6^{3-/4-}$ and 0.1 M KCl.

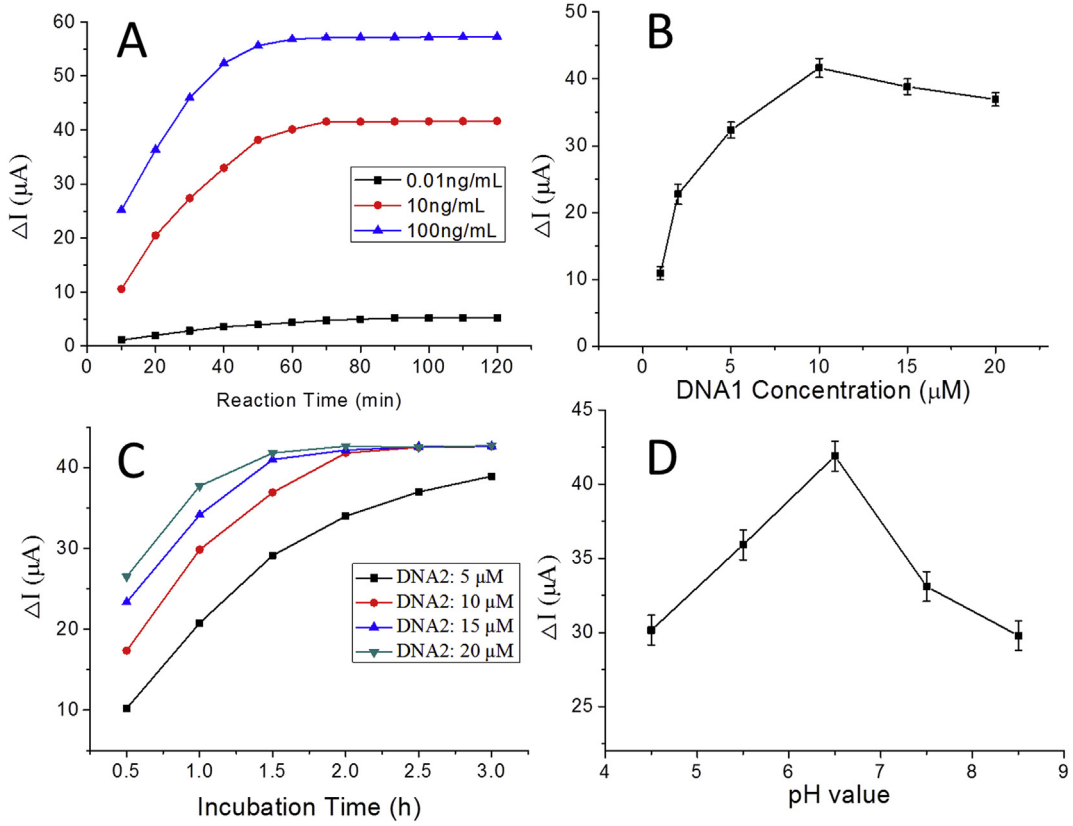

Fig. 9. The optimization of (A) Reaction time with different concentrations of β-LG and aptamer; (B) DNA 1 concentration; (C) Incubation time of the DNA2/Au@$BiVO_4$ probe with the DNA1/Au/ITO working electrode at different concentration of DNA2; (D) pH value of the detection system. The concentration of β-LG was 10 ng mL^{-1} in (B), (C) and (D).

connected to the electrode through the hybridization of DNA1 and DNA2, leading to a greater current signal. From the calibration plot (Fig. 10(B)), we can see the good linear relationship between △I (△I =Ic_n-Ic_0, c_n = 0.01–1000 ng mL^{-1}) and the logarithm of the concentration of β-LG in the range of 0.01–1000 ng mL^{-1} (△I = 5.9307ln$C_{β\text{-}LG}$ +29.695, R^2 = 0.992), with a limit of detection (LOD) of 0.007 ng mL^{-1} ($LOD = 3\delta = 3\sqrt{\frac{\sum(I_{0i}-\bar{I}_0)}{n-1}}/5.93$, I_0 is the signal of blank sample). This result was comparable with the performance of existing detection methods (Table 1), illustrating the good potential of this system for practical application.

3.6. The selectivity, reproducibility and stability of the biosensor

We investigated the selectivity of the biosensor toward several other proteins (Fig. 11). The concentration of β-LG was 10 ng mL^{-1}, while the concentration of the added interfering proteins was 1 μg mL^{-1} in all cases. It can be seen from the figure that the electrochemical signal of the interfering proteins was very small even when the concentration was 100-fold that of β-LG, which shows that the selectivity of the biosensor is acceptable. The reproducibility and stability of the as-prepared biosensor were also investigated under the optimal conditions. We prepared five electrodes in parallel, and tested them using a sample solution containing 10 ng mL^{-1} of β-LG.

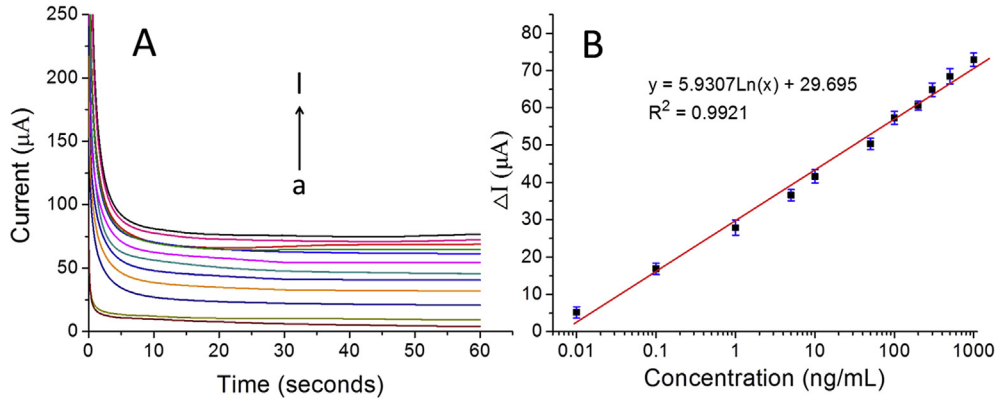

Fig. 10. (A) Amperometric i-t curves of β-LG at 0, 0.01, 0.1, 1, 5, 10, 50, 100, 200, 300, 500 and 1000 ng mL^{-1} (from a to l) and (B) linear relationship between △I and $lnC_{β\text{-}LG}$. (Potential: 0.3 V; Electrolyte: 0.5 mM TMB, 0.5 mM H_2O_2, 0.1 M PB, pH 6.5).

Table 1
Comparison of the performance characteristics of published β-LG determination methods with the biosensor developed in this study.

Methods	Linear range (ng mL^{-1})	LOD (ng mL^{-1})	Reference
Electrochemistry	0.1–100	0.02	[11]
ELISA	31.25–6.4×10^4	0.49	[30]
Fluorometric method	0.25–50	0.037	[31]
ELISA	$0.49–1.6 \times 10^4$	0.12	[32]
Immunochromatography	none	500	[4]
ELISA	$78–1 \times 10^4$	114	[8]
ELISA	$31.25–8 \times 10^3$	1.96	[9]
Visualized microarray	none	50	[6]
Immunodetection	none	500	[7]
Electrochemistry	$0.01–1 \times 10^3$	0.007	This work

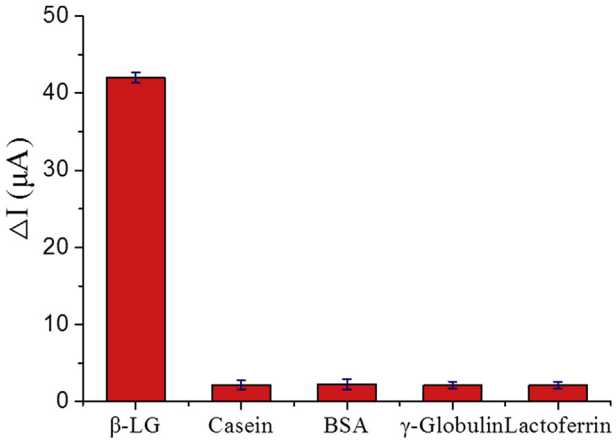

Fig. 11. The selectivity of the biosensor towards other proteins.

As can be seen in Fig. 12(A), the relative standard deviation (RSD) of the five electrodes was 2.59%, which indicated that the reproducibility of the biosensor is acceptable. The concentration of β-LG in the stability experiment was also 10 ng mL^{-1}. Since the reproducibility of the biosensor is acceptable, we prepared four working electrodes (Aptamer/DNA1/AuNPs/ITO electrode) and DNA2/Au@$BiVO_4$ probe in parallel to indirectly investigate the stability of the biosensor. The prepared probe was divided into four parts. Except for the one that needs to be used immediately, the remaining three electrodes and three parts of probe were all stored in Tris-acetate buffer (10 mM, pH 8.0) at −20 °C until further use. As shown in Fig. 12 (B), the signal response remained at 88.6% of the initial value after 30 days, which indicated that the sensor has a certain level of stability.

3.7. Analysis of samples

To further investigate the sensor's potential application, different concentrations of β-LG in spiked infant food formula were determined using the proposed biosensor. The pH of the sample solution was adjusted to 6.5 with phosphate buffer. The samples were also analyzed by commercial sELISA kit (CUSABIO, USA) for comparison. As can be seen in Table 2, the recovery of the proposed biosensor was between 92.0% and 103.3% with an acceptably low RSD (≤5.4%). There was no β-LG be found in samples 1–3 by commercial sELISA kit because of the detection range of it was 0.156–10 μg mL^{-1} (156-1 × 10^4 μg mL^{-1}). For other samples the results of the proposed biosensor were in agreement with ELISA analysis. The correlation between the electrochemical biosensor and commercial sELISA kit was not less than 98.0%, indicated that the proposed biosensor was reliable with a low detection limit and had good potential application for real samples.

4. Conclusions

In this work, we developed a novel electrochemical biosensor for the detection of β-LG. The proposed biosensor based on a DNA aptamer is simple, portable, and inexpensive, avoiding the using of expensive antibodies. To the best of our knowledge, this is the first report of using flower-like $BiVO_4$ as peroxidase mimetic nanoenzyme to amplify the signal of electrochemical probe. The wide linear range of 0.01–1000 ng mL^{-1}, with a low LOD of 0.007 ng mL^{-1} and high selectivity, indicated a good potential application of our sensor in actual use.

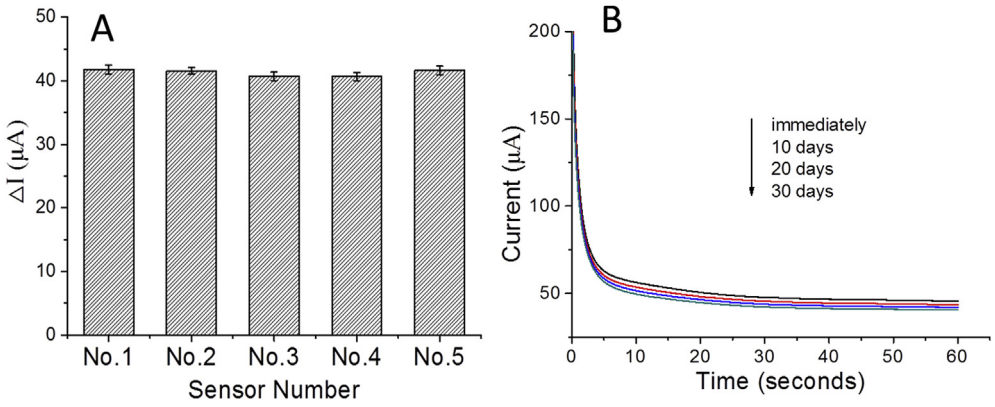

Fig. 12. The reproducibility (A) and stability (B) of the biosensor.

Table 2
Determination of β-LG in spiked infant food formula.

Sample	Spiked (ng mL^{-1})	This electrochemical biosensor (n = 5)			Commercial sELISA kit (n = 3)			Correlation (%)
		Found (ng mL^{-1})	Recovery (%)	RSD (%)	Found (ng mL^{-1})	Recovery (%)	RSD (%)	$\frac{\text{the proposed sensor}}{\text{sELISA}} \times 100$ %
1	1	0.92 ± 0.05	92.0	5.4	–			
2	10	9.4 ± 0.4	94.0	4.3	–			
3	100	95 ± 4	95.0	4.2	–			
4	200	207 ± 11	103.5	5.3	209 ± 9	104.5	4.3	99.0
5	500	481 ± 16	96.2	3.3	491 ± 17	98.2	3.5	98.0
6	1000	1015 ± 18	101.5	1.8	1020 ± 18	102.0	1.8	99.5

Declaration of competing interest

The authors declare that they have no known competing financial interests or personal relationships that could have appeared to influence the work reported in this paper.

CRediT authorship contribution statement

Shengpan Xu: Conceptualization, Methodology, Resources, Writing - original draft. **Benlin Dai:** Data curation, Software. **Wei Zhao:** Validation, Formal analysis. **Ling Jiang:** Writing - review & editing, Supervision. **He Huang:** Funding acquisition.

Acknowledgements

This work was supported by the National Key R&D Program of China (2017YFC1600404), the National Science Foundation of China (31922070, U1603112), the Natural Science Foundation of Jiangsu Province (BK20180038, BK20171461), the Six Talent Peaks Project in Jiangsu Province (2015-JY-009), the Jiangsu Synergetic Innovation Center for Advanced Bio-Manufacture (XTE1838) and Jiangsu Key Laboratory for Chemistry of Low-Dimensional Materials (JSKC19020).

Appendix A. Supplementary data

Supplementary data to this article can be found online at https://doi.org/10.1016/j.aca.2020.04.066.

References

[1] S.L. Hefle, J.A. Nordlee, S.L. Taylor, Allergenic foods, Crit. Rev. Food Sci. 36 (1996) 69–89.
[2] J.Y. Yin, J.S. Huo, X.X. Ma, J. Sun, J. Huang, Study on the simultaneously quantitative detection for β-Lactoglobulin and lactoferrin of cow milk by using protein chip technique, Biomed, Environ. Sci. 30 (2017) 875–886.
[3] Y. Ren, Z. Han, X. Chu, J. Zhang, Z. Cai, Y. Wu, Simultaneous determination of bovine α-lactalbumin and β-lactoglobulin in infant formulae by ultra-high-performance liquid chromatography–mass spectrometry, Anal. Chim. Acta 667 (2010) 96–102.
[4] P. Galan-Malo, S. Pellicer, M.D. Pérez, L. Sánchez, P. Razquin, L. Mata, Development of a novel duplex lateral flow test for simultaneous detection of casein and β-lactoglobulin in food, Food Chem. 293 (2019) 41–48.
[5] H.E. Indyk, S. Hart, T. Meerkerk, B.D. Gill, D.C. Woollard, The β-lactoglobulin content of bovine milk: development and application of a biosensor immunoassay, Int. Dairy J. 73 (2017) 68–73.
[6] Z. Li, F. Wen, Z. Li, N. Zheng, J. Jiang, D. Xu, Simultaneous detection of α-Lactoalbumin, β-Lactoglobulin and lactoferrin in milk by visualized microarray, BMC Biotechnol. 17 (2017) 72.
[7] C. Ricciardi, K. Santoro, S. Stassi, C. Lamberti, M.G. Giuffrida, M. Arlorio, L. Decastelli, Microcantilever resonator arrays for immunodetection of β-lactoglobulin milk allergen, Sensor. Actuator. B Chem. 254 (2018) 613–617.
[8] J. Orcajo, M. Lavilla, I. Martínez-de-Marañón, Specific and sensitive ELISA for measurement of IgE-binding variations of milk allergen β-lactoglobulin in processed foods, Anal. Chim. Acta 1052 (2019) 163–169.
[9] S. He, X. Li, J. Gao, P. Tong, H. Chen, Development of sandwich ELISA for testing bovine β-lactoglobulin allergenic residues by specific polyclonal antibody against human IgE binding epitopes, Food Chem. 227 (2017) 33–40.
[10] R. Zhang, N. Lu, J. Zhang, R. Yan, J. Li, L. Wang, N. Wang, M. Lv, M. Zhang, Ultrasensitive aptamer-based protein assays based on one-dimensional core-shell nanozymes, Biosens. Bioelectron. 150 (2020) 111881.
[11] S. Eissa, M. Zourob, In vitro selection of DNA aptamers targeting β-lactoglobulin and their integration in graphene-based biosensor for the detection of milk allergen, Biosens. Bioelectron. 91 (2017) 169–174.
[12] S. Xu, X. Chen, G. Peng, L. Jiang, H. Huang, An electrochemical biosensor for the detection of Pb^{2+} based on G-quadruplex DNA and gold nanoparticles, Anal. Bioanal. Chem. 410 (2018) 5879–5887.
[13] S. Xu, B. Dai, J. Xu, L. Jiang, H. Huang, An electrochemical sensor for the detection of Cu^{2+} based on gold nanoflowers-modifed electrode and DNAzyme functionalized Au@MIL-101 (Fe), Electroanalysis 31 (2019) 2330–2338.
[14] Z. Mazouz, M. Mokni, N. Fourati, C. Zerrouki, F. Barbault, M. Seydou, R. Kalfat, N. Yaakoubi, A. Omezzine, A. Bouslema, A. Othmane, Computational approach and electrochemical measurements for protein detection with MIP-based sensor, Biosens. Bioelectron. 151 (2020) 111978.
[15] D. Hu, Y. Hu, T. Zhan, Y. Zheng, P. Ran, X. Liu, Z. Guo, W. Wei, S. Wang, Co-enzyme A-aptamer-facilitated label-free electrochemical stripping strategy for sensitive detection of histone acetyltransferase activity, Biosens. Bioelectron. 150 (2020) 111934.
[16] L. Wang, X. Peng, H. Fu, C. Huang, Y. Li, Z. Liu, Recent advances in the development of electrochemical aptasensors for detection of heavy metals in food, Biosens. Bioelectron. 147 (2020) 111777.
[17] J. Shang, M. Zhao, H. Qu, H. Li, S. Chen, Fabrication of CQDs/MoS_2/Mo foil for

the improved electrochemical detection, Anal. Chim. Acta 1079 (2019) 79–85.
[18] A. Bharti, S. Rana, D. Dahiya, N. Agnihotri, N. Prabhakar, An electrochemical aptasensor for analysis of MUC1 using gold platinum bimetallic nanoparticles deposited carboxylated graphene oxide, Anal. Chim. Acta 1097 (2020) 186–195.
[19] M.R.Y. Veera, B. Sravani, H. Maseed, T. Łuczak, M. Osińska, L. SubramanyamSarma, V.V.S.S. Srikanth, G. Madhavi, Ultrafine Pt–Ni bimetallic nanoparticles anchored on reduced graphene oxide nanocomposites for boosting electrochemical detection of dopamine in biological samples, New J. Chem. 42 (2018) 16891–16901.
[20] M.R.Y. Veera, S. Bathinapatla, T. Łuczak, M. Osińska, H. Maseed, P. Ragavendra, L. Subramanyam Sarma, V.V.S.S. Srikanth, G. Madhavi, An ultra-sensitive electrochemical sensor for the detection of acetaminophen in the presence of etilefrine using bimetallic Pd–Ag/reduced graphene oxide nanocomposites, New J. Chem. 42 (2018) 3137–3146.
[21] B. Sravani, H. Maseed, Y. Chandrasekhar, M.R.Y. Veera, V.V.S.S. Srikanth, G. Madhavi, L. Subramanyam Sarma, A Pt-free graphenaceous composite as an electro-catalyst for efficient oxygen reduction reaction, Nanoscale 11 (2019) 13300–13308.
[22] H. Lv, Y. Li, X. Zhang, Z. Gao, C. Zhang, S. Zhang, Y. Dong, Enhanced peroxidase-like properties of Au@Pt DNs/NG/Cu^{2+} and application of sandwich-type electrochemical immunosensor for highly sensitive detection of CEA, Biosens. Bioelectron. 112 (2018) 1–7.
[23] S. Su, Y. Wu, D. Zhu, J. Chao, X. Liu, Y. Wan, Y. Su, X. Zuo, C. Fan, L. Wang, On-electrode synthesis of shape-controlled hierarchical flower-like gold nanostructures for efficient interfacial DNA assembly and sensitive electrochemical sensing of microRNA, Small 12 (2016) 3794–3801.
[24] W. Zhao, X. Tu, X. Wang, B. Dai, L. Zhang, J. Xu, Y. Feng, N. Ni, F. Zhu, Novel p-n heterojunction photocatalyst fabricated by flower-like $BiVO_4$ and Ag_2S nanoparticles: simple synthesis and excellent photocatalytic performance, Chem. Eng. J. 361 (2019) 1173–1181.
[25] G. Peng, X. Li, F. Cui, Q. Qiu, X. Chen, H. Huang, Aflatoxin B1 electrochemical aptasensor based on tetrahedral DNA nanostructures functionalized three dimensionally ordered macroporous MoS2–AuNPs film, ACS Appl. Mater. Interfaces 10 (2018) 17551–17559.
[26] W. Zhao, Y. Feng, J. Zhang, F. Zhu, Z. Sheng, B. Dai, D.Y.C. Leung, L. Zhang, J. Xu, Novel Ag/p-AgBr/n-$BiVO_4$ plasmonic heterojunction photocatalyst: study on the excellent photocatalytic performance and photocatalytic mechanism, ACS Appl. Energy Mater. 2 (2019) 694–704.
[27] Y. Huang, M. Zhao, S. Han, Z. Lai, J. Yang, C. Tan, Q. Ma, Q. Lu, J. Chen, X. Zhang, Growth of Au nanoparticles on 2D metalloporphyrinic metal-organic framework nanosheets used as biomimetic catalysts for cascade reactions, Adv. Mater. 29 (2017) 1700102.
[28] J.M. Song, Y.Z. Lin, H.B. Yao, F.J. Fan, X.G. Li, S.H. Yu, Superlong β-$AgVO_3$ nanoribbons: high-yield synthesis by a pyridine-assisted solution approach, their stability, electrical and electrochemical properties, ACS Nano 3 (2009) 653–660.
[29] C.W. Lien, C.C. Huang, H.T. Chang, Peroxidase-mimic bismuth–gold nanoparticles for determining the activity of thrombin and drug screening, Chem. Commun. 48 (2012) 7952–7954.
[30] S. He, X. Li, Y. Wu, S. Wu, Z. Wu, A. Yang, P. Tong, J. Yuan, J. Gao, H. Chen, A novel sandwich enzyme-linked immunosorbent assay with covalently bound monoclonal antibody and gold probe for sensitive and rapid detection of bovine β-lactoglobulin, Anal. Bioanal. Chem. 410 (2018) 3693–3703.
[31] M. Shi, Y. Cen, M. Sohail, G. Xu, F. Wei, Y. Ma, X. Xu, Y. Ma, Y. Song, Q. Hu, Aptamer based fluorometric β-lactoglobulin assay based on the use of magnetic nanoparticles and carbon dots, Microchim. Acta 185 (2017) 40.
[32] S. He, X. Li, Y. Wu, S. Wu, Z. Wu, A. Yang, P. Tong, J. Yuan, J. Gao, H. Chen, Highly sensitive detection of bovine β-Lactoglobulin with wide linear dynamic range based on platinum nanoparticles probe, J. Agric. Food Chem. 66 (2018) 11830–11838.